IOP FTC
IOP PUBLISHING SMART MATERIALS AND STRUCTURES
Smart Mater. Struct. **21** (2012) 082001 (8pp) doi:10.1088/0964-1726/21/8/082001

FAST TRACK COMMUNICATION

Array of piezoelectric energy harvesting by the equivalent impedance approach

I C Lien and Y C Shu[1]

Institute of Applied Mechanics, National Taiwan University, Taipei 106, Taiwan, Republic of China

E-mail: yichung@iam.ntu.edu.tw

Received 27 February 2012, in final form 20 June 2012
Published 24 July 2012
Online at stacks.iop.org/SMS/21/082001

Abstract
This article proposes to use the idea of equivalent impedance to investigate the electrical response of an array of piezoelectric oscillators endowed with distinct energy harvesting circuits. Three interface electronics systems are considered including standard AC/DC and parallel/series-SSHI (synchronized switch harvesting on inductor) circuits. Various forms of equivalent load impedance are analytically obtained for different interfaces. The steady-state response of an array system is then shown to be determined by the matrix formulation of generalized Ohm's law whose impedance matrix is explicitly expressed in terms of the load impedance. A model problem is proposed for evaluating the ability of power harvesting under various conditions. It is shown first that harvested power is increased dramatically for the case of small deviation in the system parameters. On the other hand, if the deviation in mass is relatively large, the result is changed from the power-boosting mode to wideband mode. In particular, the parallel-SSHI array system exhibits much more significant bandwidth improvement than the other two cases. Surprisingly, the series-SSHI array system shows the worst electrical response. Such an observation is opposed to our previous finding that an SSHI technique avails against the standard technique in the case based on a single piezoelectric energy harvester and the explanation is under investigation.

1. Introduction

Vibration-based piezoelectric energy harvesting has received significant attention recently due to the potential of high energy density capable of powering remote sensor nodes [3, 5–7, 16, 34, 42]. It is superior to other vibration-to-electricity conversions because of possessing high electromechanical coupling, no external voltage source requirement, and the ease of implementation in MEMS and nanosystems [12, 26, 27, 30, 32, 46]. Precisely, a real device includes oscillators for transmitting ambient vibrations to strain energy which is converted into electric energy through the direct piezoelectric effect. The harvested charges are accumulated through a suitable interface circuit and are presented to loads.

Typically, a power generator is designed as a resonant oscillator and the cantilever beam configuration is widely chosen for transverse excitation bases [4, 11, 28, 35]. While such a design has enjoyed great success in power harvesting, there are two inherent drawbacks. The first is the small power area density, and therefore, the increase in harvested power requires enlarging areas which may be prohibited due to the limitation in the size of device. The second is the significant power reduction at off-resonance. This motivates a number of research efforts to develop an array of piezoelectric energy harvesters for power boosting and bandwidth improvement. Several research attempts have been carried out in designing multi-tier cantilever-beam-based power generators [8, 9, 36, 40, 43, 45]. However, their results either lack of analysis or are only valid for AC power output in spite of the ultimate need for DC output. Hence, there is a need for developing a suitable methodology to study this complicated problem [22].

This article investigates the electrical behavior of an array of piezoelectric energy harvesters endowed with several

[1] Author to whom any correspondence should be addressed.

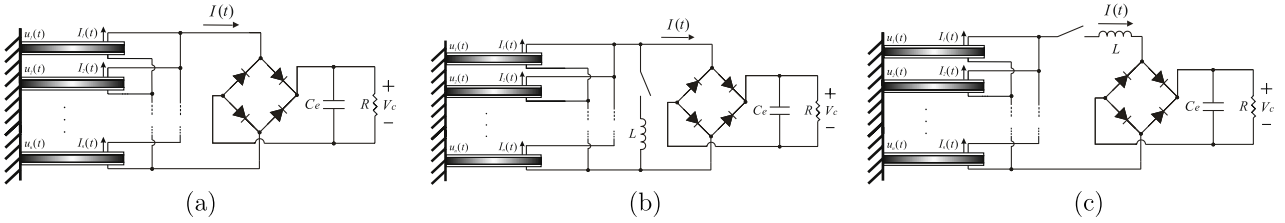

Figure 1. An array of piezoelectric energy harvesters connected in parallel. It is connected to a standard interface as in (a), a parallel-SSHI interface as in (b), and a series-SSHI interface as in (c).

interfacing circuits, including the standard AC/DC circuit and parallel/series-SSHI (synchronized switch harvesting on inductor) circuits. While the analysis of these interface circuits in the case of a single piezoelectric oscillator has been studied in several research works [1, 10, 15, 17, 18, 24, 25, 33, 37–39, 41], the extension to the case of multiple piezoelectric oscillators has not been done yet. Here, we develop a methodology based on the idea of equivalent impedance to approach this problem. Notice that the use of impedance analysis and matching theory for optimal power transfer in the case of piezoelectric energy harvesting is not new and has been proposed by several research works. This includes the complex impedance analysis for AC power output [2, 20, 31] and the resistive impedance matching circuit for DC power output [13, 14, 29]. However, recently Liang and Liao [19] have pointed out that these studies either do not consider the real energy harvesting circuits or neglect the reaction of power conditioning circuits to the dynamics of the mechanical part. They have further provided an in-depth analysis accounting for these factors to study the equivalent impedance of a piezoelectric energy harvesting system. Our approach is similar to theirs except that they choose the first Fourier mode of circuit waveforms for impedance analysis [19]. As a result, the explicit expression of equivalent impedance is hard to obtain due to the difficulty in solving trigonometric equations. From this there also arises the problem of extending their approach to the case of multiple piezoelectric oscillators. On the other hand, we remove such an approximation on the circuit waveforms and derive the explicit expression of equivalent load impedance and, therefore, it is feasible to extend our approach to the case of an array of piezoelectric oscillators connected in parallel. Indeed, let the velocity vector and force vector both be multiplied by certain suitable constants analogous to the current vector and voltage vector, respectively. We show that they are related by the generalized Ohm's law whose matrix of impedance is formulated analytically in terms of the load impedance. The harvested average power generated by the array system is therefore obtained by inverting this matrix formulation.

Finally, a model problem consisting of three piezoelectric oscillators is proposed for investigating the ability in power harvesting for different interface circuits. The electrical response is shown to change significantly depending on the various extents of deviation in the system parameters of oscillators. It also varies dramatically for different choices of energy harvesting circuits linked to the system. A certain unexpected phenomenon is found and is in contrast with what was observed in the case based on the resonant vibration of a single piezoelectric oscillator.

2. Model

Consider an array of piezoelectric oscillators connected in parallel as shown in figure 1. Suppose the parameters of each piezoelectric oscillator do not deviate significantly. Further suppose the modal density of each vibrator is widely separated and the array structure is vibrating at around the resonance frequency. In this case, we may model the array system as a mass + spring + damper + piezostructure with governing equations described by [37]

$$M_n\ddot{u}_n(t) + \eta_n\dot{u}_n(t) + K_n u_n(t) + \Theta_n V_{p_n}(t) = F_n(t), \tag{1}$$

$$-\Theta_n\dot{u}_n(t) + C_{p_n}\dot{V}_{p_n}(t) = -I_n(t), \tag{2}$$

$$F_n(t) = F_n\sin(wt + \tau_n), \tag{3}$$

where $n = 1, 2, \ldots, N$ and N is the total number of oscillators, u_n the displacement of the nth mass M_n, V_{p_n} the voltage across the nth piezoelectric element, $F_n(t)$ the forcing function applied to the nth oscillator and $I_n(t)$ the current flowing into the specified circuit. In addition, in equations (1) and (2), η_n, K_n, Θ_n and C_{p_n} are the mechanical damping coefficient, the stiffness, the piezoelectric coefficient and the capacitance of the nth piezoelectric oscillator. The forcing function $F_n(t)$ is assumed to be harmonic with w as the angular frequency (in radians per second) and τ_n as the given phase shift angle. We also use F_n as the magnitude of harmonic excitation to save notation in the future development. Next, as the array system is connected in parallel $V_p = V_{p_n}$ for all n. Thus, equation (2) can be rewritten as

$$-I^*(t) + C_p\dot{V}_p(t) = -I(t), \tag{4}$$

where

$$I^*(t) = \sum_{n=1}^{N}\Theta_n\dot{u}_n(t), \qquad C_p = \sum_{n=1}^{N}C_{p_n}, \qquad I(t) = \sum_{n=1}^{N}I_n(t). \tag{5}$$

Suppose the array of oscillators is connected to a standard circuit consisting of a rectifier followed by a filtering capacitance C_e for AC/DC conversion, as illustrated in figure 1(a). The terminal load is represented by a resistor R

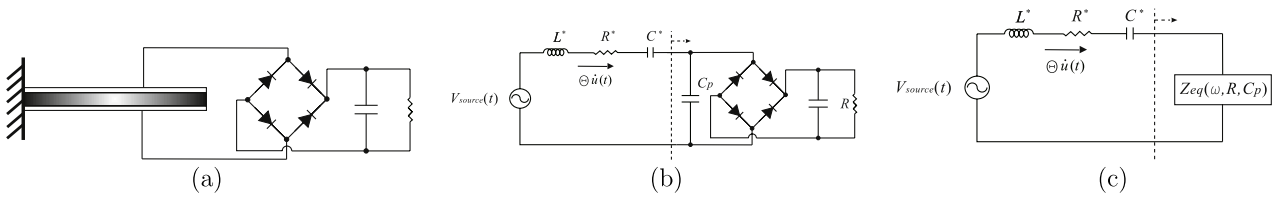

Figure 2. A single piezoelectric oscillator connected to a standard interface. (a) A schematic of this system. (b) An equivalent circuit model of this system. (c) An equivalent impedance added for replacing the piezoelectric capacitance and the energy harvesting circuit.

and V_c is the DC voltage across it, as also shown in figure 1(a). The rectifying bridge is assumed to be perfect here. Let I_0^* be the magnitude of $I^*(t)$ under the steady-state operation. Its relation with the DC voltage V_c can be obtained by integrating the equation of charge balance from equation (4) over the semi-period of oscillation. This gives

$$V_c^{\text{Standard}} = \left(\frac{R}{\frac{\pi}{2} + C_p R w}\right) I_0^*. \tag{6}$$

Indeed, the derivation of equation (6) can be obtained following steps similar to those used in deriving equation (7) in [37]. The details will be revealed elsewhere [21].

Consider another case where the interface circuit is replaced with an SSHI circuit. It consists of adding up a switching device in parallel (series) with the piezoelectric array structure, as shown in figure 1(b) for parallel-SSHI and in figure 1(c) for series-SSHI. The electronic switch is triggered at the vanishing points of $I^*(t)$. As a result, this gives various degrees of inversion in the piezoelectric voltage $V_p(t)$. Following the techniques developed by [39] (see equation (12) therein) and [24] (see equation (13) therein), the magnitude of piezoelectric current source and the terminal DC voltage are related by

$$V_c^{\text{P-SSHI}} = \frac{2R}{(1 - q_I) C_p R w + \pi} I_0^* \tag{7}$$

for the parallel-SSHI and

$$V_c^{\text{S-SSHI}} = \frac{2R(1 + q_I)}{\pi(1 - q_I) + 2C_p R w (1 + q_I)} I_0^* \tag{8}$$

for the series-SSHI [21]. In the above, $q_I = \mathrm{e}^{-\frac{\pi}{2Q_I}}$ and Q_I is the electrical quality factor introduced in the SSHI circuits for measuring the extent of energy loss from the inductor in series with the switch [10, 39]. Finally, the harvested average power P is

$$P = \frac{V_c^2}{R}, \tag{9}$$

and the goal here is to find out the explicit form of it for different energy harvesting circuits.

3. Idea of equivalent impedance

Consider a single piezoelectric oscillator endowed with a standard AC/DC energy harvesting circuit, as shown in figure 2(a). Thus, $N = 1$ in equations (1)–(3) which can be transformed into an equivalent circuit model with $R^* = \frac{\eta}{\Theta^2}$ as resistance, $L^* = \frac{M}{\Theta^2}$ as inductance, $C^* = \frac{\Theta^2}{K}$ as capacitance and $V_{\text{source}} = \frac{F}{\Theta}$ as the voltage source, as shown in figure 2(b) [24, 39, 44]. The subscript 1 is neglected for simplicity. Let Z_{eq} be the equivalent impedance of the circuit elements consisting of the piezoelectric capacitance C_p and the harvesting circuit, as illustrated in figure 2(c). Therefore, the voltage and current passing through Z_{eq} are V_p and $\Theta\dot{u}$. They are related by

$$V_p = (\Theta\dot{u})\, Z_{\text{eq}}. \tag{10}$$

The steady-state solution of this circuit for $F(t) = \bar{F}\mathrm{e}^{\mathrm{j}wt}$ can be obtained by setting

$$u(t) = \bar{u}\mathrm{e}^{\mathrm{j}wt}, \qquad V_p = \bar{V}_p \mathrm{e}^{\mathrm{j}wt}, \tag{11}$$

where $\mathrm{j}^2 = -1$. Substituting these two into equations (1) and (10) gives

$$\bar{u} = \frac{\bar{F}}{(-w^2 M + K - w\Theta^2 Z_{\text{I}}) + \mathrm{j}w(\eta + \Theta^2 Z_{\text{R}})}, \qquad Z_{\text{eq}} = Z_{\text{R}} + \mathrm{j}Z_{\text{I}}, \tag{12}$$

where Z_{R} and Z_{I} are the real and imaginary parts of the complex impedance Z_{eq}. Thus, the magnitude of displacement is

$$|\bar{u}| = \frac{\bar{F}}{\{(-w^2 M + K - w\Theta^2 Z_{\text{I}})^2 + (w\eta + w\Theta^2 Z_{\text{R}})^2\}^{\frac{1}{2}}}. \tag{13}$$

The determination of the impedance Z_{eq} can be achieved as follows. First, the analytic steady-state solution of equations (1)-(3) for a piezoelectric oscillator connected to the standard interface has been proposed by Shu and Lien (equation (28) in [37])

$$|\bar{u}| = \frac{\bar{F}}{\{(-w^2 M + K + \frac{w\Theta^2 R}{\frac{\pi}{2} + C_p w R})^2 + (w\eta + \frac{2w\Theta^2 R}{(\frac{\pi}{2} + C_p w R)^2})^2\}^{\frac{1}{2}}}. \tag{14}$$

Thus, the comparison between equation (13) and equation (14) gives

$$Z_{\text{R}}^{\text{Standard}} = \frac{2R}{\left(\frac{\pi}{2} + C_p R w\right)^2}, \qquad Z_{\text{I}}^{\text{Standard}} = -\frac{R}{\left(\frac{\pi}{2} + C_p R w\right)}. \tag{15}$$

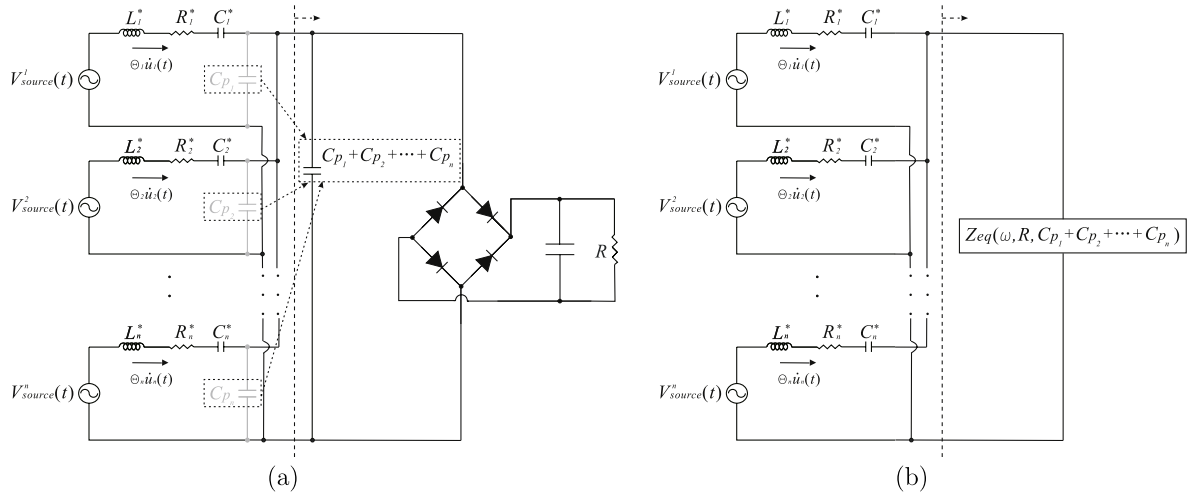

Figure 3. An array of piezoelectric oscillators connected in parallel and endowed with a standard energy harvesting circuit. (a) An equivalent circuit model of this array system. (b) An equivalent impedance added for replacing the piezoelectric capacitance and the energy harvesting circuit.

Next, if the interface circuit is changed to the parallel/series-SSHI, their associated equivalent impedance can be obtained following the approach similar to the previous case of a standard circuit. Indeed, the comparison of magnitude of displacement between equation (13) and equation (19) in [39] gives the equivalent impedance for the parallel-SSHI case

$$Z_{\mathrm{R}}^{\mathrm{P-SSHI}} = \frac{2[1+\frac{(1-q_I^2)}{2\pi}C_pRw]R}{(\frac{\pi}{2}+\frac{(1-q_I)}{2}C_pRw)^2}, \qquad Z_{\mathrm{I}}^{\mathrm{P-SSHI}} = \frac{-\frac{(1-q_I)}{2}R}{(\frac{\pi}{2}+\frac{(1-q_I)}{2}C_pRw)}, \tag{16}$$

and the comparison between equation (13) and equation (19) in [24] gives the equivalent impedance for the series-SSHI case

$$Z_{\mathrm{R}}^{\mathrm{S-SSHI}} = \frac{4(1+q_I)}{[\pi(1-q_I)+2(1+q_I)C_pRw]wC_p}, \qquad Z_{\mathrm{I}}^{\mathrm{S-SSHI}} = \frac{-1}{C_pw}. \tag{17}$$

4. Generalized Ohm's law

Let us return to the case of multiple piezoelectric energy harvesters connected in parallel. Suppose this array system is connected to a standard energy harvesting circuit as shown in figure 1(a). Similar to the case of a single oscillator, its equivalent circuit model can be presented as in figure 3(a), where $R_n^* = \frac{\eta_n}{\Theta_n^2}$ as resistance, $L_n^* = \frac{M_n}{\Theta_n^2}$ as inductance, $C_n^* = \frac{\Theta_n^2}{K_n}$ as capacitance, and $V_{\mathrm{source}}^n = \frac{F_n}{\Theta_n}$ as the voltage source [24, 39, 44]. Since all the oscillators are connected in parallel, the overall piezoelectric capacitance is $C_p = \sum_{n=1}^N C_{pn}$, as also illustrated in figure 3(a). Following the approach developed in section 3, let Z_{eq} represent the equivalent impedance of the elements consisting of C_p and the energy harvesting circuit, as shown in figure 3(b). This gives

$$V_p = \left(\sum_{n=1}^N \Theta_n\dot{u}_n\right) Z_{\mathrm{eq}}, \tag{18}$$

where V_p and $(\sum_{n=1}^N \Theta_n\dot{u}_n)$ are the piezoelectric voltage and net current crossing Z_{eq} whose expression is given by equation (15) for the standard interface.

To solve the steady-state solution under the excitation function $F_n = \bar{F}_n e^{\mathrm{j}(wt+\tau_n)}$, set $u_n = \bar{u}_n e^{\mathrm{j}(wt+\tau_n+\theta_n)}$ where θ_n are the unknown phase shifts. Thus, from equation (1) and equation (18), we have

$$\left[\frac{-w^2M_n+K_n}{w\Theta_n^2}+\mathrm{j}\frac{\eta_n}{\Theta_n^2}\right](w\Theta_n\bar{u}_ne^{\mathrm{j}(\tau_n+\theta_n)}) + \mathrm{j}\left[\sum_{n=1}^N w\Theta_n\bar{u}_ne^{\mathrm{j}(\tau_n+\theta_n)}\right]Z_{\mathrm{eq}} = \frac{\bar{F}_ne^{\mathrm{j}\tau_n}}{\Theta_n}. \tag{19}$$

If we set

$$\hat{V}_n = \frac{\bar{F}_ne^{\mathrm{j}\tau_n}}{\Theta_n}, \qquad \hat{I}_n = \mathrm{j}w\Theta_n\bar{u}_ne^{\mathrm{j}(\tau_n+\theta_n)}, \qquad n=1,\ldots,N, \tag{20}$$

this gives the generalized Ohm's law in the matrix form,

$$\hat{\mathbf{V}} = \hat{\mathbf{Z}}\hat{\mathbf{I}}, \qquad \hat{\mathbf{V}} = \left(\hat{V}_n\right), \qquad \hat{\mathbf{I}} = \left(\hat{I}_n\right) \tag{21}$$

where $\hat{\mathbf{Z}}$ is the generalized impedance matrix given by

$$\hat{Z}_{kl} = \begin{cases} \dfrac{\eta_k}{\Theta_k^2}+Z_{\mathrm{eq}}+\mathrm{j}\dfrac{wM_k}{\Theta_k^2}-\mathrm{j}\dfrac{K_k}{w\Theta_k^2} & \text{if } k=l, \\ Z_{\mathrm{eq}} & \text{if } k\neq l. \end{cases} \tag{22}$$

Note that from equation (5), $I^*(t) = \sum_{n=1}^N \Theta_n\dot{u}_n(t) = \sum_{n=1}^N \mathrm{j}w\Theta_n\bar{u}_ne^{\mathrm{j}(\tau_n+\theta_n)}e^{\mathrm{j}wt}$. Hence from equation (6) and

equation (20), the magnitude of DC voltage V_c^{standard} is

$$V_c^{\text{Standard}} = \left(\frac{R}{C_pRw + \frac{\pi}{2}}\right)|I_0^*| = \left(\frac{R}{C_pRw + \frac{\pi}{2}}\right)\left|\sum_{n=1}^{N} \mathrm{j}w\Theta_n\bar{u}_n e^{\mathrm{j}(\tau_n+\theta_n)}\right| = \left(\frac{R}{C_pRw + \frac{\pi}{2}}\right)\left|\sum_{n=1}^{N}\hat{I}_n\right|, \quad (23)$$

where each $\hat{I}_n$ is obtained by inverting the matrix formulation of the generalized Ohm's law in equation (21). The harvested average power P is therefore obtained through equation (9).

Although the standard interface is chosen to illustrate how to apply the idea of equivalent impedance to study the steady-state response of an array system, it is clear this approach works for other interfaces such as SSHI circuits. Indeed, the generalized Ohm's law in equation (21) and equation (22) remains unchanged except that Z_{eq} is replaced by $Z_{\text{eq}}^{\text{P-SSHI}}$ in equation (16) for the parallel-SSHI case and replaced by $Z_{\text{eq}}^{\text{S-SSHI}}$ in equation (17) for the series-SSHI case. Therefore, from equation (7) and equation (8), the harvested DC voltage is

$$V_c^{\text{P-SSHI}} = \frac{2R}{(1-q_I)C_pRw + \pi}\left|\sum_{n=1}^{N}\hat{I}_n\right| \quad (24)$$

for the parallel-SSHI and

$$V_c^{\text{S-SSHI}} = \frac{2R(1+q_I)}{\pi(1-q_I) + 2C_pRw(1+q_I)}\left|\sum_{n=1}^{N}\hat{I}_n\right| \quad (25)$$

for the series-SSHI.

5. Results

The proposed estimates have been validated numerically through the conventional PSpice circuit simulation [23] and, therefore, provide a valuable tool for design analysis. To illustrate this, a model problem is proposed for evaluating the ability in power harvesting under various conditions. Consider a device consisting of three piezoelectric oscillators connected in parallel. Suppose they have identical system parameters except for different magnitudes of mass; i.e. $M_n = 0.006\,514\lambda_n$ kg, $\eta_n = 0.126\,28$ N s m^{-1}, $K_n = 481.207$ N m^{-1}, $\Theta_n = 0.001\,587$ N V^{-1}, $C_{p_n} = 45$ nF, $F_n = 0.045\,79$ N, $\tau_n = 0$ and $q_I = 0.3$. The parameter λ_n denotes the different degrees of deviation in mass. Three cases of different combinations of λ_n will be studied next. Before doing this, note that the electrical response of a single piezoelectric oscillator connected to the standard/parallel/series-SSHI circuits has been evaluated in [24] and therefore, their comparisons are briefly summarized below. The magnitudes of peak power are around 1.8 mW and are almost the same in these three cases since the electromechanical coupling of the oscillator is in the medium range ($\frac{k_e^2}{\zeta} \approx 3.3$, $k_e^2 = \frac{\Theta^2}{KC_p}$, $\zeta = \frac{\eta}{2\sqrt{KM}}$ for $\lambda_n = 1$). In addition, both parallel-SSHI and series-SSHI systems exhibit wider bandwidth and therefore show advantage over the standard circuit system (for example, see figures 6(b), (e) and (h) in [24]).

Consider the first case where there is no deviation in mass; i.e. $\lambda_1 = \lambda_2 = \lambda_3 = 1$. The results are shown in figure 4(a) (parallel-SSHI circuit), figure 4(b) (standard circuit) and figure 4(c) (series-SSHI circuit) where power is shown against frequency under various resistive loads. Obviously, there is a significant rise in harvested power which is boosted three times higher than that based on a single piezoelectric oscillator. The optimal load can be further shown to be reduced to one third of the original one in each case.

Next, consider the case where the deviation in mass is around 5%; i.e. $\lambda_1 = 1.05$, $\lambda_2 = 1$ and $\lambda_3 = 0.95$. It causes different resonant frequencies of oscillators. They are around 42.2 Hz, 43.3 Hz and 44.4 Hz, respectively. The results for parallel-SSHI, standard and series-SSHI array systems are shown in figures 4(d)–(f) where power is against frequency under various loads. Three observations are drawn from this simulation. First, the magnitude of optimal power is reduced to 2.5 times larger than that based on the resonant vibration of a single piezoelectric oscillator. Second, the parallel-SSHI array system exhibits a flat region in the frequency domain. In other words, it enjoys bandwidth improvement in power harvesting. However, such an effect is not obvious in the series-SSHI system. Third, figure 4(e) reveals that the peak power of the standard system is achieved at the driving frequency excited around 45 Hz which is close to the largest resonant frequency of the oscillator ($\lambda_3 = 0.95$). Such an observation reveals an important message for the design analysis of optimal power.

Consider the final case where the deviation in mass is large; i.e. $\lambda_1 = 1.09$, $\lambda_2 = 1$ and $\lambda_3 = 0.91$. The natural frequency of each piezoelectric oscillator is 41.4 Hz, 43.3 Hz and 45.4 Hz, respectively. The results for parallel-SSHI, standard and series-SSHI array systems are shown in figures 4(g)–(i), and they deliver other important messages for system design. First, the effect of power boosting is reduced and the optimal power is only 1.8 times larger than that based on a single piezoelectric energy harvester. But both the standard and parallel-SSHI array systems exhibit various extents of bandwidth improvement in power harvesting. Indeed, the standard circuit array system shows roughly three different peaks of power corresponding to the distinct resonances of component oscillators. The maximum of these peaks is driven at around the largest resonant frequency of the oscillator ($\lambda_3 = 0.91$). On the other hand, the parallel-SSHI array system exhibits a remarkable wideband effect in power harvesting. Finally, much to our surprise, the present series-SSHI array system shows an unexpected electric response. In fact, under the assumption of ideal diodes, SSHI systems based on a single piezoelectric oscillation have been shown to possess much wider inherent bandwidth than the standard circuit system [24], but such an ability of bandwidth improvement turns out to be lost in the series-SSHI array system. The explanation is unknown and is under investigation.

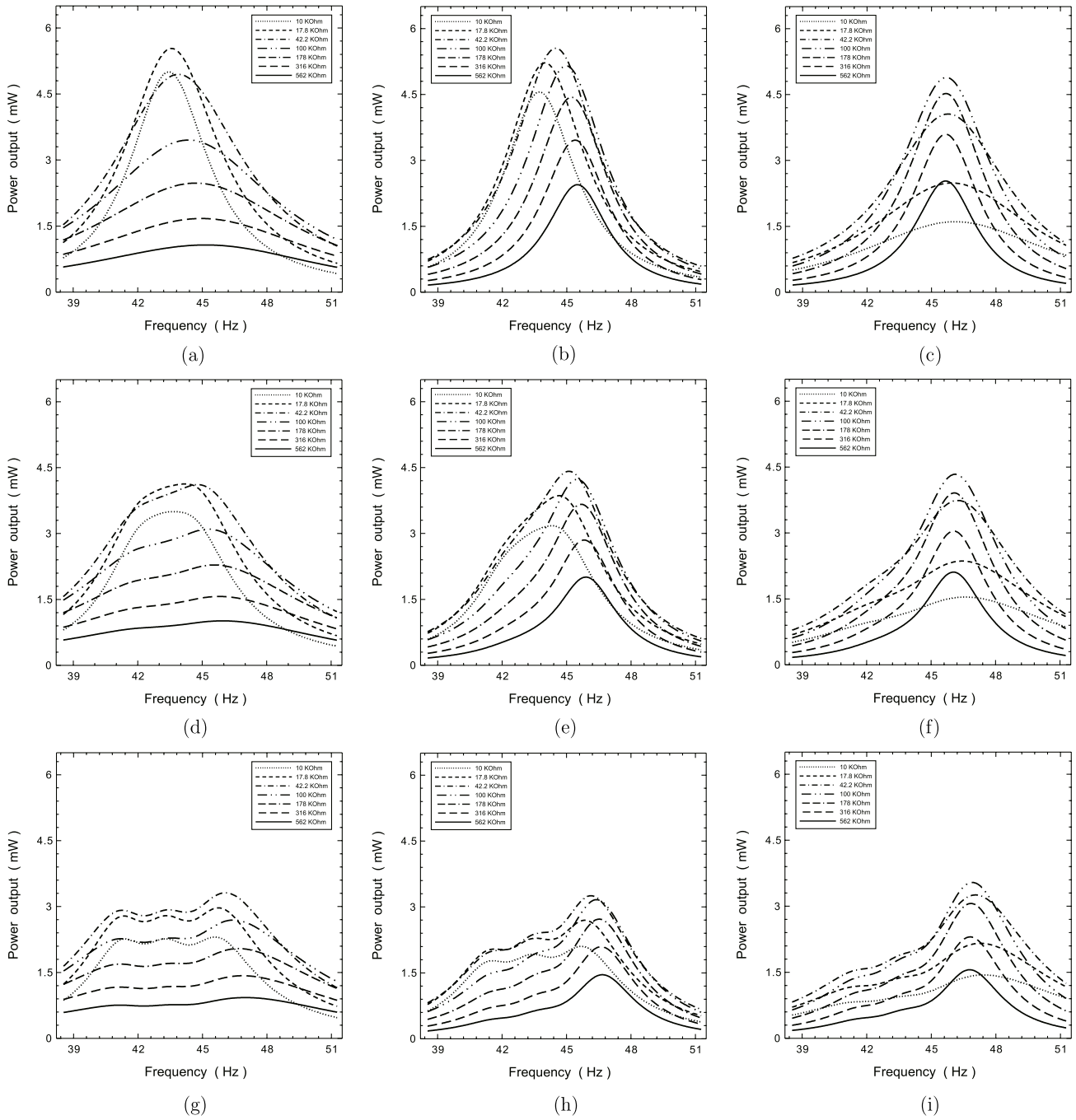

Figure 4. Harvested power of an array of piezoelectric oscillators connected to different interface electronics. It is plotted against frequency under different values of resistance. (a), (d) and (g) are for the parallel-SSHI interface, (b), (e) and (h) are for the standard interface and (c), (f) and (i) are for the series-SSHI interface. In addition, (a)–(c) indicate the case of identical system parameters; (d)–(f) indicate the case of small deviation in mass; (g)–(i) indicate the case of large deviation in mass.

6. Conclusion

This article investigates the electrical response of an array of piezoelectric oscillators connected in parallel and attached to various energy harvesting circuits, including the standard and parallel/series-SSHI interfaces. The methodology is based on the consideration of impedance of piezoelectric capacitance coupled with different interfaces. The main result is the formulation of generalized Ohm's law in equation (21) whose impedance matrix is derived explicitly in terms of load impedance as in equation (22). The system behavior is then determined by the inversion of this matrix formulation.

A model problem based on an array of three piezoelectric oscillators is proposed for the performance evaluation of power harvesting for different interface circuits. First, DC power output increases significantly if the deviations in the system parameters are small. However, if the deviations are relatively large, power output changes from the power-

boosting mode to wideband mode. In addition, the parallel-SSHI array system exhibits much more significant bandwidth improvement than the other two cases. Surprisingly, it is found that the electrical response of a series-SSHI system does not outperform the standard circuit system. Such a result contradicts what we observed in the case of a single piezoelectric energy harvester.

Acknowledgments

The support from National Taiwan University and from National Science Council under Grant No. 99-2221-E-002-071-MY3 is appreciated.

References

[1] Badel A, Benayad A, Lefeuvre E, Lebrun L, Richard C and Guyomar D 2006 Single crystals and nonlinear process for outstanding vibration-powered electrical generators *IEEE Trans. Ultrason. Ferroelectr. Freq. Control* **53** 673–84
[2] Brufau-Penella J and Puig-Vidal M 2009 Piezoelectric energy harvesting improvement with complex conjugate impedance matching *J. Intell. Mater. Syst. Struct.* **20** 597–608
[3] Cottone F, Vocca H and Gammaitoni L 2009 Nonlinear energy harvesting *Phys. Rev. Lett.* **102** 080601
[4] duToit N E, Wardle B L and Kim S G 2005 Design considerations for MEMS-scale piezoelectric mechanical vibration energy harvesters *Integr. Ferroelectr.* **71** 121–60
[5] Elvin N G, Lajnef N and Elvin A A 2006 Feasibility of structural monitoring with vibration powered sensors *Smart Mater. Struct.* **15** 977–86
[6] Erturk A and Inman D J 2008 Issues in mathematical modeling of piezoelectric energy harvesters *Smart Mater. Struct.* **17** 065016
[7] Erturk A and Inman D J 2011 *Piezoelectric Energy Harvesting* (New York: Wiley)
[8] Ferrari M, Ferrari V, Guizzetti M and Marioli D 2009 An autonomous battery-less sensor module powered by piezoelectric energy harvesting with RF transmission of multiple measurement signals *Smart Mater. Struct.* **18** 085023
[9] Ferrari M, Ferrari V, Guizzetti M, Marioli D and Taroni A 2008 Piezoelectric multifrequency energy converter for power harvesting in autonomous microsystems *Sensors Actuators* A **142** 329–35
[10] Guyomar D, Badel A, Lefeuvre E and Richard C 2005 Toward energy harvesting using active materials and conversion improvement by nonlinear processing *IEEE Trans. Ultrason. Ferroelectr. Freq. Control* **52** 584–95
[11] Hu H P, Cui Z J and Cao J G 2007 Performance of a piezoelectric bimorph harvester with variable width *J. Mechan.* **23** 197–202
[12] Jeon Y B, Sood R, Jeong J H and Kim S G 2005 MEMS power generator with transverse mode thin film PZT *Sensors Actuators* A **122** 16–22
[13] Kim H, Priya S, Stephanou H and Uchino K 2007 Consideration of impedance matching techniques for efficient piezoelectric energy harvesting *IEEE Trans. Ultrason. Ferroelectr. Freq. Control* **54** 1851–9
[14] Kong N, Ha D S, Erturk A and Inman D J 2010 Resistive impedance matching circuit for piezoelectric energy harvesting *J. Intell. Mater. Syst. Struct.* **21** 1293–302
[15] Lallart M and Guyomar D 2008 An optimized self-powered switching circuit for non-linear energy harvesting with low voltage output *Smart Mater. Struct.* **17** 035030
[16] Lesieutre G A, Ottman G K and Hofmann H F 2004 Damping as a result of piezoelectric energy harvesting *J. Sound Vib.* **269** 991–1001
[17] Liang J R and Liao W H 2009 Piezoelectric energy harvesting and dissipation on structural damping *J. Intell. Mater. Syst. Struct.* **20** 515–27
[18] Liang J R and Liao W H 2011 Energy flow in piezoelectric energy harvesting systems *Smart Mater. Struct.* **20** 015005
[19] Liang J R and Liao W H 2012 Impedance modeling and analysis for piezoelectric energy harvesting systems *IEEE/ASME Trans. Mechatronics* doi:10.1109/TMECH.2011.2160275
[20] Liao Y and Sodano H A 2009 Optimal parameters and power characteristics of piezoelectric energy harvesters with an RC circuit *Smart Mater. Struct.* **18** 045011
[21] Lien I C 2012 Dynamic analysis of an array of piezo-energy harvesting system endowed with various interface circuits *PhD Thesis* National Taiwan Univesity
[22] Lien I C and Shu Y C 2011 Array of piezoelectric energy harvesters *Proc. Active and Passive Smart Structures and Integrated Systems; Proc. SPIE* **7977** 79770K
[23] Lien I C and Shu Y C 2012 Multiple piezoelectri energy harvesters connected to different interface circuits *Proc. Active and Passive Smart Structures and Integrated Systems; Proc. SPIE* **8341** 83410X
[24] Lien I C, Shu Y C, Wu W J, Shiu S M and Lin H C 2010 Revisit of series-SSHI with comparisons to other interfacing circuits in piezoelectric energy harvesting *Smart Mater. Struct.* **19** 125009
[25] Liu Y, Tian G, Wang Y, Lin J, Zhang Q and Hofmann H F 2009 Active piezoelectric energy harvesting: general principle and experimental demonstration *J. Intell. Mater. Syst. Struct.* **20** 575–85
[26] Majdoub M S, Sharma P and Cagin T 2008 Enhanced size-dependent piezoelectricity and elasticity in nanostructures due to the flexoelectric effect *Phys. Rev.* B **77** 125424
[27] Mitcheson P D, Yeatman E M, Rao G K, Holmes A S and Green T C 2008 Energy harvesting from human and machine motion for wireless electronic devices *Proc. IEEE* **96** 1457–86
[28] Mo C, Kim S and Clark W W 2009 Theoretical analysis of energy harvesting performance for unimorph piezoelectric benders with interdigitated electrodes *Smart Mater. Struct.* **18** 055017
[29] Ottman G K, Hofmann H F, Bhatt A C and Lesieutre G A 2002 Adaptive piezoelectric energy harvesting circuit for wireless remote power supply *IEEE Trans. Power Electron.* **17** 669–76
[30] Qin Y, Wang X and Wang Z L 2008 Microfibre-nanowire hybrid structure for energy scavenging *Nature* **451** 809–13
[31] Renno J M, Daqaq M F and Inman D J 2009 On the optimal energy harvesting from a vibration source *J. Sound Vib.* **320** 386–405
[32] Roundy S, Wright P K and Rabaey J 2003 A study of low level vibrations as power source for wireless sensor nodes *Comput. Commun.* **26** 1131–44
[33] Rupp C J, Dunn M L and Maute K 2010 Analysis of piezoelectric energy harvesting systems with non-linear circuits using the harmonic balance method *J. Intell. Mater. Syst. Struct.* **21** 1383–96
[34] Scruggs J T 2009 An optimal stochastic control theory for distributed energy harvesting networks *J. Sound Vib.* **320** 707–25
[35] Seuaciuc-Osorio T and Daqaq M F 2009 On the reduced-order modeling of energy harvesters *J. Intell. Mater. Syst. Struct.* **20** 2003–16

[36] Shahruz S M 2006 Design of mechanical band-pass filters with large frequency bands for energy scavenging *Mechatronics* **16** 523–31
[37] Shu Y C and Lien I C 2006 Analysis of power output for piezoelectric energy harvesting systems *Smart Mater. Struct.* **15** 1499–512
[38] Shu Y C and Lien I C 2006 Efficiency of energy conversion for a piezoelectric power harvesting system *J. Micromech. Microeng.* **16** 2429–38
[39] Shu Y C, Lien I C and Wu W J 2007 An improved analysis of the SSHI interface in piezoelectric energy harvesting *Smart Mater. Struct.* **16** 2253–64
[40] Song H J, Choi Y T, Purekar A S and Wereley N M 2009 Performance evaluation of multi-tier energy harvesters using macro-fiber composite patches *J. Intell. Mater. Syst. Struct.* **20** 2077–88
[41] Wickenheiser A M and Garcia E 2010 Power optimization of vibration energy harvesters utilizing passive and active circuits *J. Intell. Mater. Syst. Struct.* **21** 1343–61
[42] Wu W J, Wickenheiser A M, Reissman T and Garcia E 2009 Modeling and experimental verification of synchronized discharging techniques for boosting power harvesting from piezoelectric transducers *Smart Mater. Struct.* **18** 055012
[43] Xue H, Hu Y T and Wang Q M 2008 Broadband piezoelectric energy harvesting devices using multiple bimorphs with different operating frequencies *IEEE Trans. Ultrason. Ferroelectr. Freq. Control* **55** 2104–8
[44] Yang Y and Tang L 2009 Equivalent circuit modeling of piezoelectric energy harvesters *J. Intell. Mater. Syst. Struct.* **20** 2223–35
[45] Yang Z and Yang J 2009 Connected vibrating piezoelectric bimorph beams as a wide-band piezoelectric power harvester *J. Intell. Mater. Syst. Struct.* **20** 569–74
[46] Yen T T, Hirasawa T, Wright P K, Pisano A P and Lin L 2011 Corrugated aluminum nitride energy harvesters for high energy conversion effectiveness *J. Micromech. Microeng.* **21** 085037